Available online at www.sciencedirect.com
SCIENCE DIRECT®
Journal of Hydrology 277 (2003) 268–279
Journal of Hydrology
www.elsevier.com/locate/jhydrol

Steady groundwater flow through many cylindrical inhomogeneities in a multi-aquifer system

Mark Bakker*

Department of Biological and Agricultural Engineering, University of Georgia, Athens, GA 30602, USA

Received 26 April 2002; accepted 13 March 2003

Abstract

A new approach is presented for the simulation of steady-state groundwater flow in multi-aquifer systems that contain many cylindrical inhomogeneities. The hydraulic conductivity of all aquifers and the resistance of all leaky layers may be different inside each cylinder. The approach is based on separation of variables and combines principles of the theory for multi-aquifer flow with principles of the analytic element method. The solution fulfills the governing differential equations exactly everywhere; the head, flow, and leakage between aquifers may be computed analytically at any point in the aquifer system. The boundary conditions along the circumference of the cylinder are satisfied approximately, but may be met at any precision. Two examples are discussed to illustrate the accuracy of the approach and the significance of inhomogeneities in multi-aquifer systems. The first application simulates the vertical and horizontal, advective spreading of a conservative tracer in a homogeneous aquifer that is overlain by an aquifer with cylindrical inclusions of higher permeability. The second application concerns the three-dimensional shape of the capture zone of a well that is screened in the bottom aquifer of a three-aquifer system. The capture zone extends to the top aquifer due to cylindrical holes of lower resistance in the separating clay layers.

Keywords: Multi-aquifer; Inhomogeneities; Analytic element method; Capture zone

1. Introduction

The objective of this paper is to present a new analytic element approach for the simulation of steady-state groundwater flow through multi-aquifer systems that contain many cylindrical inhomogeneities. The proposed approach may be used, for example, to study the effect on the flow of local inclusions of higher or lower hydraulic conductivity, or to study the effect of holes in leaky separating layers. If the exact location and properties of such inclusions and holes are unknown, the approach may be used for hypothesis-testing, based on available hydrogeological evidence of the discontinuity of aquifer properties, leaky layer properties, or both. The hydraulic conductivity of all aquifers and the resistance of all leaky layers may be different inside each cylinder, but the cylinders may not overlap; flow must remain (semi)confined in all aquifers. Two examples are presented to illustrate the significance of inhomogeneities in multi-aquifer systems. The first example is the advective spreading of a conservative tracer

* Fax: +1-706-542-8806.
E-mail address: mbakker@engr.uga.edu (M. Bakker).

0022-1694/03/$ - see front matter
doi:10.1016/S0022-1694(03)00128-8

in a homogeneous aquifer that is overlain by an aquifer with cylindrical inclusions of higher permeability. The second example studies the extent of the capture zone of a pumping well in a system of homogeneous aquifers with leaky clay layers that contain sandy, cylindrical holes.

The general theory for steady-state flow through an aquifer system consisting of an arbitrary number of aquifers and leaky layers was first presented by Hemker (1984). Maas (1986) demonstrated the power of matrix equations to solve flow in semi-confined, multi-aquifer systems. Bruggeman (1999) used this approach to derive exact solutions to over 50 problems of semi-confined, multi-aquifer flow, including several problems of radial flow through a single cylindrical inhomogeneity. Exact solutions for uniform flow through a single cylindrical inhomogeneity in a confined aquifer system were presented by Bakker (2002).

The analytic element formulation for steady-state flow through cylindrical inhomogeneities in a single aquifer was developed by Strack (1987, 1989). Barnes and Janković (1999) developed algorithms for the accurate computation of the coefficients in the solution and the efficient modeling of flow through a large number of cylinders. Strack (1989) also presented a theory for flow through elliptical inhomogeneities in a single aquifer. An analogous theory for three-dimensional flow through ellipsoidal inhomogeneities was developed by Fitts (1991); accurate and efficient algorithms to simulate flow through thousands of ellipsoids were presented by Janković and Barnes (1999).

The approach presented in this paper is based on the separation of variables and applies principles of the theory for multi-aquifer flow of Hemker (1984) and the analytic element method (Strack, 1989; Haitjema, 1995). Use will be made of algorithms developed by Barnes and Janković (1999) to increase accuracy and efficiency. The solution will fulfill the governing systems of differential equations exactly everywhere. It will be possible to compute the head, flow, and leakage between aquifers analytically at any point in the aquifer system. The boundary conditions along the circumference of the cylinder will be satisfied approximately, but to any desired accuracy, depending on the abilities of the employed computer.

2. Basic equations for multi-aquifer flow

Consider a confined, multi-aquifer system with M aquifers and $M+1$ leaky layers (Fig. 1); leaky layers 1 and $M+1$ are impermeable. The aquifers are numbered 1 through M from top to bottom and the leaky layers are numbered 1 (top of aquifer 1) through $M+1$ (bottom of aquifer M). All aquifer properties are homogeneous and isotropic, and are written as vectors of which component m represents layer m (following the notation of Hemker, 1984; Maas, 1986; and Bruggeman, 1999). The transmissivities of the aquifers are represented by the vector $\vec{T}$ [L^2/T] and the resistances to vertical flow of the leaky layers by the vector $\vec{C}$ [T]; since the aquifer system is confined, $C_1 = C_{M+1} = \infty$. The comprehensive transmissivity of the aquifer system, the sum of the transmissivities of all aquifers, is called T, and the normalized unit transmissivity vector is defined as $\vec{T}_n = \vec{T}/T$. A cylindrical r, θ, z coordinate system is adopted (Fig. 1).

The resistance to flow in the vertical direction is neglected within an aquifer (the Dupuit–Forchheimer approximation). It is emphasized that this does not mean that flow in the aquifer is horizontal. The vertical component of flow may be obtained at any point in the aquifer from three-dimensional continuity of flow, once the horizontal components are computed (Polubarinova-Kochina, 1962, p. 408; Strack, 1984). Flow in the leaky layers is approximated as vertical. The upward leakage q_p [L/T] from aquifer p to aquifer $p-1$ is computed as

$$q_p = (h_p - h_{p-1})/C_p \tag{1}$$

where h_p is the head in aquifer p. Steady-state flow in aquifer p is governed by (e.g. Hemker, 1984)

$$\nabla^2(T_p h_p) = \frac{h_p - h_{p-1}}{C_p} + \frac{h_p - h_{p+1}}{C_{p+1}} \tag{2}$$

where ∇^2 is the two-dimensional Laplacian. The heads in the differential equation may be converted to discharge potentials (Strack, 1989), and the differential equations for all aquifers may be combined into one matrix differential equation (e.g. Hemker, 1984)

$$\nabla^2 \vec{\Phi} = \mathbf{G}\vec{\Phi} \tag{3}$$

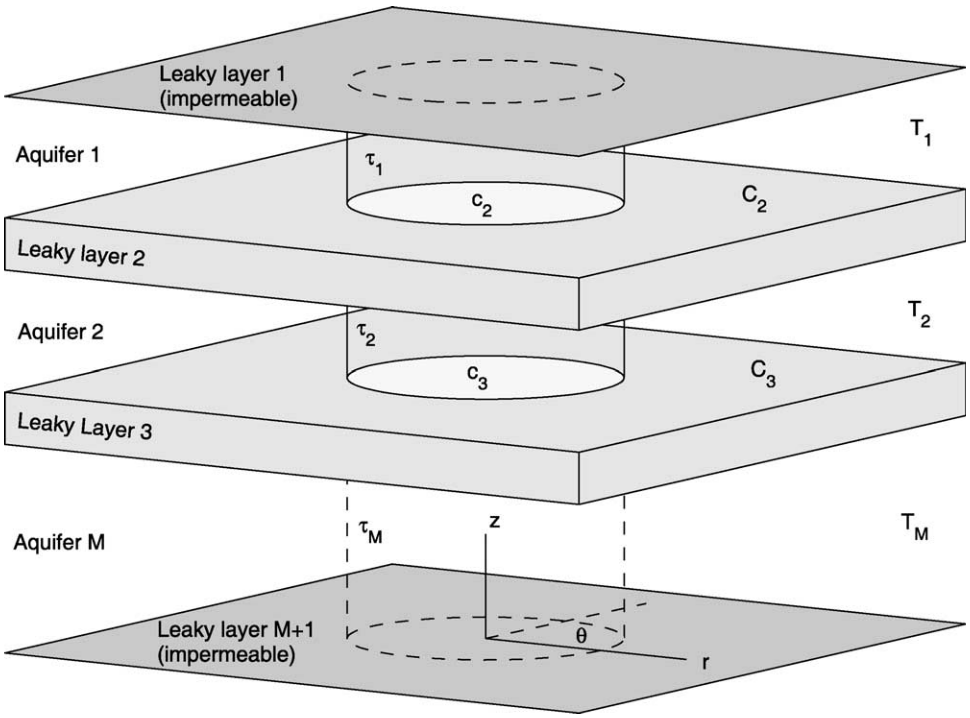

Fig. 1. A multi-aquifer system with a cylindrical inhomogeneity; shaded portions represent leaky layers.

where $\vec{\Phi}$ is a column-vector of discharge potentials

$$\vec{\Phi} = \vec{T} \odot \vec{h} \tag{4}$$

where '$\odot$' stands for the term-by-term multiplication of two vectors (the Hadamard product; e.g. Magnus and Neudecker, 1999). **G** is the system matrix, a tri-diagonal $M \times M$ matrix with diagonal terms

$$G_{m,m} = \frac{1}{C_m T_m} + \frac{1}{C_{m+1} T_m} \tag{5}$$

and off-diagonal terms

$$G_{m,m-1} = \frac{-1}{C_m T_{m-1}} \qquad G_{m,m+1} = \frac{-1}{C_{m+1} T_{m+1}} \tag{6}$$

The r and θ components of the discharge vector, the vertically integrated flow in each aquifer, are each written as column vectors, with their components representing the r and θ components of flow in the different aquifers. The components of the discharge vector may be obtained from the potential by differentiation

$$\vec{Q}_r = -\frac{\partial \vec{\Phi}}{\partial r} \qquad \vec{Q}_\theta = -\frac{1}{r}\frac{\partial \vec{\Phi}}{\partial \theta} \tag{7}$$

For a confined aquifer system consisting of M aquifers, the system matrix is semi-positive definite and has $M-1$ positive eigenvalues and one zero eigenvalue. The non-zero eigenvalues are called w_m ($m = 1, \ldots, M-1$) and the corresponding eigenvectors $\vec{U}_m$. The general solution to Eq. (3) may be written as (e.g. Hemker, 1984; Bakker and Strack, 2003)

$$\vec{\Phi} = F_L \vec{T}_n + \sum_{m=1}^{M-1} F_m \vec{U}_m \tag{8}$$

where F_L fulfills Laplace's differential equation in two dimensions

$$\nabla^2 F_L = 0 \tag{9}$$

and F_m fulfills the modified Helmholtz equation

$$\nabla^2 F_m = F_m / \Lambda_m^2 \tag{10}$$

where $\Lambda_m = 1/\sqrt{w_m}$ are called the leakage factors and have the dimension of length. It is important to note that for a confined aquifer system, the sum of the components of each eigenvector $\vec{U}_m$ equals zero (Bakker, 2001), and thus F_L is the comprehensive potential, the sum of the potentials in all aquifers (e.g. Strack, 1981).

3. Problem statement

Consider a confined aquifer system with a cylindrical inhomogeneity in a general flow field (which may contain other cylindrical inhomogeneities); the cylinder cuts through all aquifers and leaky layers (Fig. 1). The origin of an r, θ, z coordinate system is chosen at the center of the cylinder on the bottom of the bottom aquifer; θ is measured counter-clockwise and the z axis points vertically upward. The aquifer properties on the outside of the cylinder are as stated previously (they are also summarized in Table 1). On the inside of the cylinder, the transmissivity vector is $\vec{\tau}$, the comprehensive transmissivity is τ, the normalized unit transmissivity vector is $\vec{\tau}_n$, and the vector of resistances of the leaky layers is $\vec{c}$; the radius of the cylinder is R.

Table 1
Basic notation

Aquifer properties	
M	Number of aquifers
$\vec{T}$	Transmissivity vector outside cylinder
$\vec{\tau}$	Transmissivity vector inside cylinder
T	Comprehensive transmissivity of aquifer system outside cylinder $T = \sum T_i$
τ	Comprehensive transmissivity of aquifer system inside cylinder $\tau = \sum \tau_i$
$\vec{T}_n$	Normalized transmissivity vector outside cylinder $\vec{T}_n = \vec{T}/T$
$\vec{\tau}_n$	Normalized transmissivity vector inside cylinder $\vec{\tau}_n = \vec{\tau}/\tau$
$\vec{C}$	Resistance vector outside cylinder.
$\vec{c}$	Resistance vector inside cylinder
System matrix symbols	
$\mathbf{G}$	System matrix outside cylinder
$\mathbf{H}$	System matrix inside cylinder
w_m	Non-zero eigenvalue m of $\mathbf{G}$
ω_m	Non-zero eigenvalue m of $\mathbf{H}$
$\vec{U}_m$	Eigenvector m of $\mathbf{G}$ corresponding to non-zero eigenvalue w_m
$\vec{V}_m$	Eigenvector m of $\mathbf{H}$ corresponding to non-zero eigenvalue ω_m
Λ_m	Leakage factor m outside cylinder $\Lambda_m = 1/\sqrt{w_m}$
λ_m	Leakage factor m inside cylinder $\lambda_m = 1/\sqrt{\omega_m}$

The vector of discharge potentials on the inside of the cylinder is defined as

$$\vec{\Phi} = \vec{\tau} \odot \vec{h} \tag{11}$$

Steady-state flow on the inside of the cylinder is governed by

$$\nabla^2 \vec{\Phi} = \mathbf{H}\vec{\Phi} \tag{12}$$

The coefficients of the system matrix $\mathbf{H}$ may be obtained with Eqs. (5) and (6) when the components of the vectors $\vec{T}$ and $\vec{C}$ are replaced with the components of the vectors $\vec{\tau}$ and $\vec{c}$, respectively. The non-zero eigenvalues of $\mathbf{H}$ are called ω_m ($m = 1, \ldots, M-1$), the corresponding leakage factors $\lambda_m = 1/\sqrt{\omega_m}$, and the corresponding eigenvectors $\vec{V}_m$.

The boundary conditions along the circumference of the cylinder are that the head and radial flow are continuous in each aquifer

$$\vec{h}^+ = \vec{h}^- \tag{13}$$

$$\vec{Q}_r^+ = \vec{Q}_r^- \tag{14}$$

where the superscripts '+' and '−' stand for evaluation on the circumference of the cylinder ($r = R$) just inside and just outside the cylinder, respectively. The former condition may be written in terms of potentials as

$$\vec{\Phi}^+ \odot \vec{T} - \vec{\Phi}^- \odot \vec{\tau} = 0 \tag{15}$$

The potential due to the cylinder is called $\vec{\Phi}_c$ and must fulfill Eq. (12) on the inside of the cylinder and Eq. (3) on the outside of the cylinder, and must have enough degrees of freedom to satisfy boundary conditions (14) and (15) accurately along the circumference of the cylinder. In addition, the potential due to the cylinder must be finite everywhere and should vanish at infinity.

4. Solution

The potential in the aquifer system on the outside of the cylinder is written as

$$\vec{\Phi} = \vec{\Phi}_c + \vec{\Phi}_o \qquad r \geq R \tag{16}$$

where $\vec{\Phi}_c$ is the vector of discharge potentials due to the cylinder, and $\vec{\Phi}_o$ is the vector of discharge potentials due to all other aquifer features (which may include other cylinders). On the inside of the cylinder, $\vec{\Phi}_o$ is not valid because it does not fulfill Eq. (12), and the potential is written instead as

$$\vec{\Phi} = \vec{\Phi}_c + \Phi_o \vec{\tau}_n \qquad r \le R \tag{17}$$

where Φ_o is the comprehensive potential of $\vec{\Phi}_o$ (i.e. the portion that fulfills Laplace's equation); Φ_o is a function of the horizontal coordinates only.

Following Eq. (8), $\vec{\Phi}_c$ will be written on the outside of the cylinder as

$$\vec{\Phi}_c = F_L \vec{T}_n + \sum_{m=1}^{M-1} F_m \vec{U}_m \qquad r \ge R \tag{18}$$

and on the inside as

$$\vec{\Phi}_c = G_L \vec{\tau}_n + \sum_{m=1}^{M-1} G_m \vec{V}_m \qquad r \le R \tag{19}$$

where F_L and G_L fulfill Laplace's differential equation, and F_m and G_m fulfill the modified Helmholtz equations

$$\nabla^2 F_m = F_m / \Lambda_m^2 \tag{20}$$

$$\nabla^2 G_m = G_m / \lambda_m^2 \tag{21}$$

Expressions for F_L, F_m, G_L, and G_m will be obtained by application of separation of variables.

5. Separation of variables

The general solution Φ_L to Laplace's equation in cylindrical coordinates may be written as follows, using separation of variables (Moon and Spencer (1971), p. 14)

$$\Phi_L(r, \theta) = (Ar^p + Br^{-p})[C\cos(p\theta) + D\sin(p\theta)] \tag{22}$$

where p is a non-negative integer. Since F_L must be finite on the outside of the cylinder and vanish at infinity, it only includes negative powers of p

$$F_L = \sum_{p=1}^{\infty} [a_p \cos(p\theta) + b_p \sin(p\theta)] r^{-p} \tag{23}$$

The function G_L must be finite on the inside of the cylinder, and thus does not include any negative powers of r

$$G_L = \sum_{p=0}^{\infty} [\alpha_p \cos(p\theta) + \beta_p \sin(p\theta)] r^p \tag{24}$$

The modified Hemlholtz equation in r and θ may also be solved using separation of variables. Moon and Spencer (1971, p. 16) show that separation of the unmodified Hemlholtz equation (i.e. Eq. (10) has a negative term on the right-hand side), results in Bessel's differential equation in r. The separated modified-Helmholtz equation may be obtained through the addition of a negative sign to the results of Moon and Spencer, which results in the modified Bessel's differential equation in r (as may be expected). The general solution may be written as

$$\Phi_m = [A\mathrm{I}_p(r/l_m) + B\mathrm{K}_p(r/l_m)][C\cos(p\theta) + D\sin(p\theta)] \tag{25}$$

where I_p and K_p are modified Bessel functions of order p and of the first and second kind, respectively, and l_m is a leakage factor. Recall that $\mathrm{I}_p(r)$ approaches zero for r approaching zero (except I_0 which approaches one), and I_p approaches infinity for r approaching infinity (e.g. Abramowitz and Stegun, 1965). Conversely, $\mathrm{K}_p(r)$ approaches infinity for r approaching zero, and zero for r approaching infinity. Since F_m must be finite on the outside of the cylinder and vanish at infinity, it does not contain any functions I_p

$$F_m = \sum_{p=0}^{\infty} [c_p \cos(p\theta) + d_p \sin(p\theta)] \mathrm{K}_p(r/\Lambda_m) \tag{26}$$

The functions G_m must be finite on the inside of the cylinder and thus do not contain any functions K_p

$$G_m = \sum_{p=0}^{\infty} [\gamma_p \cos(p\theta) + \delta_p \sin(p\theta)] \mathrm{I}_p(r/\lambda_p) \tag{27}$$

The potential due to a cylindrical inhomogeneity may now be obtained by combining Eqs. (18), (19), (23), (24), (26) and (27). For practical purposes, the infinite series are truncated at $p = P$, which will be referred to as the order of the inhomogeneity.

The potential on the outside of the cylinder is

$$\vec{\Phi}_{\mathrm{c}} = \sum_{p=1}^{P} [a_p \cos(p\theta) + b_p \sin(p\theta)] r^{-p} \vec{T}_n + \sum_{m=1}^{M-1} \sum_{p=0}^{P} [c_{p,m} \cos(p\theta) + d_{p,m} \sin(p\theta)] \mathrm{K}_{\mathrm{p}}(r/\Lambda_m) \vec{U}_m \quad (28)$$

and on the inside of the cylinder

$$\vec{\Phi}_{\mathrm{c}} = \sum_{p=0}^{P} [\alpha_p \cos(p\theta) + \beta_p \sin(p\theta)] r^{p} \vec{\tau}_n + \sum_{m=1}^{M-1} \sum_{p=0}^{P} [\gamma_{p,m} \cos(p\theta) + \delta_{p,m} \sin(p\theta)] \mathrm{I}_{\mathrm{p}}(r/\lambda_m) \vec{V}_m \quad (29)$$

The coefficients $d_{0,m}$, β_0, and $\delta_{0,m}$ all equal zero (because $\sin(p\theta)$ vanishes for $p=0$). The other coefficients will be determined by application of the boundary conditions as discussed in Section 6. Expressions of the r and θ components of the discharge vector may be obtained from differentiation of the discharge potential, and are presented in the Appendix. It is noted that the portions of the solutions that fulfill Laplace's equation (Eqs. (23) and (24)) are equivalent to the real part of the solution for a circular inhomogeneity in a single aquifer presented by Strack (1987), who formulated his problem in terms of a complex potential.

6. Solving for the coefficients

The expressions for the potential due to the cylindrical inhomogeneity (Eqs. (28) and (29)) contain a total of $2M(2P+1)-1$ coefficients. The coefficients may be determined by application of the boundary conditions (14) and (15) at a number of points, referred to as collocation points, along the circumference of the cylinder. At every (x, y) location of a collocation point, boundary conditions (14) and (15) are applied in each aquifer, resulting in $2M$ linear equations per collocation point. If $2P+1$ collocation points are selected, then boundary conditions (14) and (15) may be applied at every collocation point in every aquifer, except for at one collocation point in one aquifer where only one of the two boundary conditions may be applied. The resulting system of $2M(2P+1)-1$ linear equations may be solved with a standard method.

It is emphasized that the proposed solution fulfills the governing differential equations exactly and fulfills the boundary conditions along the edge of the cylinder approximately, although up to any desired accuracy by increasing the order P. The solution for a given order P may be improved by applying the boundary conditions along the edge of the cylinder at more than $2P+1$ points, and by solving the resulting system of linear equations in a least-squares sense. The improvement in accuracy of the solution by this approach was demonstrated for cylindrical inhomogeneities in a single aquifer by Barnes and Janković (1999).

The proposed solution may be used to model flow through an aquifer system with many non-overlapping cylindrical inhomogeneities. In Eqs. (16) and (17) the potential in the aquifer was written as the sum of the potential due to a cylinder plus the potential due to all other aquifer features, potential $\vec{\Phi}_{\mathrm{o}}$, which may contain other cylindrical inhomogeneities. Hence, the values of the coefficients of one cylindrical inhomogeneity may influence the values of the coefficients of another inhomogeneity. The coefficients of all cylindrical inhomogeneities may be obtained by solving one large explicit system for all inhomogeneities simultaneously. Although this is possible, it is more convenient to compute the coefficients of each cylinder in an iterative manner, using the Gauss–Seidel approach proposed for circular inhomogeneities in single-aquifer flow by Barnes and Janković (1999). The coefficients for each cylinder are computed by holding the coefficients of all other cylinders fixed. For each cylinder, $2M(2P+1)-1$ linear equations are solved; the resulting square, full matrix may be inverted and stored using a standard approach (e.g. LDU decomposition). The final solution is obtained by cycling through all cylinders until the change of the coefficients becomes insignificant. Experimentation has shown that this approach converges quickly, generally in less than 20 iterations.

For computational accuracy it is recommended to scale the parameters by the value of the Bessel functions on the circumference of the cylinder. For example, $c_{p,m}$ in Eq. (28) should be replaced by $\tilde{c}_{p,m}/\mathrm{K}_p(R/\Lambda_m)$ and the problem should be solved for $\tilde{c}_{p,m}$. Similarly, the coefficients of the portion of the solution that fulfills Laplace's equation should be scaled according to the power of R. For example, a_p in Eq. (28) should be replaced by $\tilde{a}_p R^p$ and the problem should be solved for $\tilde{a}_p$.

7. Application I

The first application concerns the advective transport of a conservative tracer in a heterogeneous two-aquifer system. The thickness of each aquifer is 10 m and the hydraulic conductivity is 2 m/d; the leaky layer that separates the two aquifers has a thickness of 2 m and a vertical hydraulic conductivity of $k_v = 0.001$ m/d so that the vertical resistance is $C = 2000$ d. The bottom aquifer is homogeneous, but the top aquifer contains seven cylindrical inclusions with a larger hydraulic conductivity of 10 m/d; the vertical hydraulic conductivity of the leaky layer below the cylinders is $k_v = 0.04$ m/d for a resistance of $c = 50$ d. The radii of the cylinders vary from 50 to 80 m and their distribution is shown in Fig. 2. Far away from the cylinders, flow is uniform from West to East with a gradient of 0.01. It is emphasized that the hydraulic conductivity inside the cylinders in the bottom aquifer may also be varied; it is not varied here to study the specific effect of inhomogeneities in the top aquifer on the flow in the bottom aquifer.

There is one leaky layer and thus one leakage factor. Outside the cylinders the leakage factor is 141 m, inside the cylinders the leakage factor is 29 m. (From a practical standpoint, the leakage between aquifers may be considered negligible at a distance of three times the leakage factor away from any disturbances.) The order of each cylinder is chosen as $P = 4$; the influence of the order on the accuracy of the solution will be evaluated next.

A small computer program is written in MATLAB to obtain a solution. Contour lines of the head in the top and bottom aquifers are presented in Fig. 2(a) and (b), respectively (North–South running solid lines). The accuracy of the solution is evaluated by calculating the error in the normal discharge across the circumferences of the cylinders. The error ε in each aquifer is computed as

$$\varepsilon = (Q_r^+ - Q_r^-)/Q_0 \tag{30}$$

where Q_0 is the uniform flow from West to East in each aquifer. The average absolute error along the circumference of the largest cylinder is $|\bar{\varepsilon}| = 0.00018$ the maximum absolute error is $|\varepsilon|_{\max} = 0.00061$. It is noted that the sum of the errors in the normal discharges in the two aquifers equals zero, so that the overall water balance is met. Although the error ε in each aquifer is small and will have no significant practical consequence, the accuracy may be increased by increasing the order P. For example, every increase of four in the order of the largest cylinder results in approximately an order of magnitude decrease of both the average and the maximum errors. As a result, for $P = 20$ the errors have reduced to $|\bar{\varepsilon}| = 9 \times 10^{-9}$ and $|\varepsilon|_{\max} = 3 \times 10^{-8}$. The error in head along the circumferences of the cylinders decreases in a similar fashion.

The influence of the cylindrical inhomogeneities in the top aquifer on the flow in the bottom aquifer is evaluated by computing pathlines of a conservative tracer that is released in the bottom aquifer. The horizontal components of the specific discharge vector are obtained by dividing the components of the integrated horizontal discharge (Eq. (7)) by the thickness of the appropriate aquifer. The vertical component of flow at the top and bottom of each aquifer may be obtained with Eq. (1). The vertical variation of q_z within an aquifer is linear, since the resistance to flow in the vertical direction within an aquifer is neglected (Strack, 1984). Pathlines are computed using a second-order predictor-corrector scheme (e.g. Barnes and Janković, 1999); special care is taken to compute accurately the intersection of a pathline with a cylinder and with the leaky layer.

A conservative tracer is released at point A over the entire thickness of the bottom aquifer (Fig. 2(b)). Pathlines are started from nine points, with vertical intervals of 1 m, starting at 1 m above the bottom of the aquifer. Pathlines are represented by the West–East running lines in Fig. 2(a)–(c). When a pathline is in the bottom aquifer, it is represented by a solid line in Fig. 2(b) and a dotted line in Fig. 2(a). When a pathline is in the top aquifer, it is represented by a solid line in Fig. 2(a) and a dotted line in Fig. 2(b).

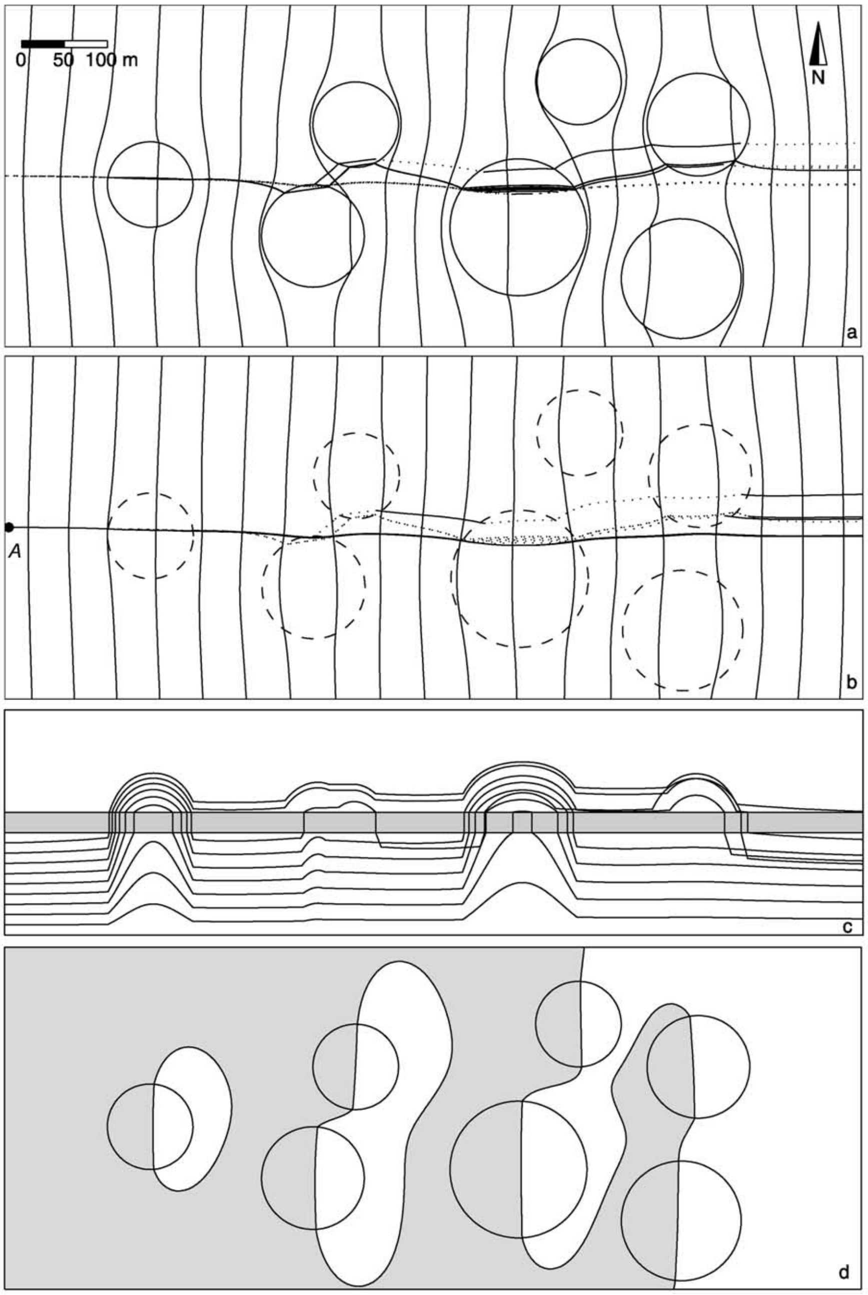

Fig. 2. Application I. (a) Pathlines in top aquifer, (b) pathlines in bottom aquifer, (c) projection of pathlines on West–East vertical cross-section (vertical scale exaggerated), and (d) areas of upward leakage (shaded).

A projection of all pathlines on a West–East running vertical cross-section is shown in Fig. 2(c), where the shaded area represents the leaky layer. To assist in the interpretation of the pathlines, areas of upward leakage through the leaky layer are shown in Fig. 2(d) (shaded areas). All but one pathline flow through portions of the top aquifer. The four pathlines with the highest starting locations (at $z = 6–9$ m)

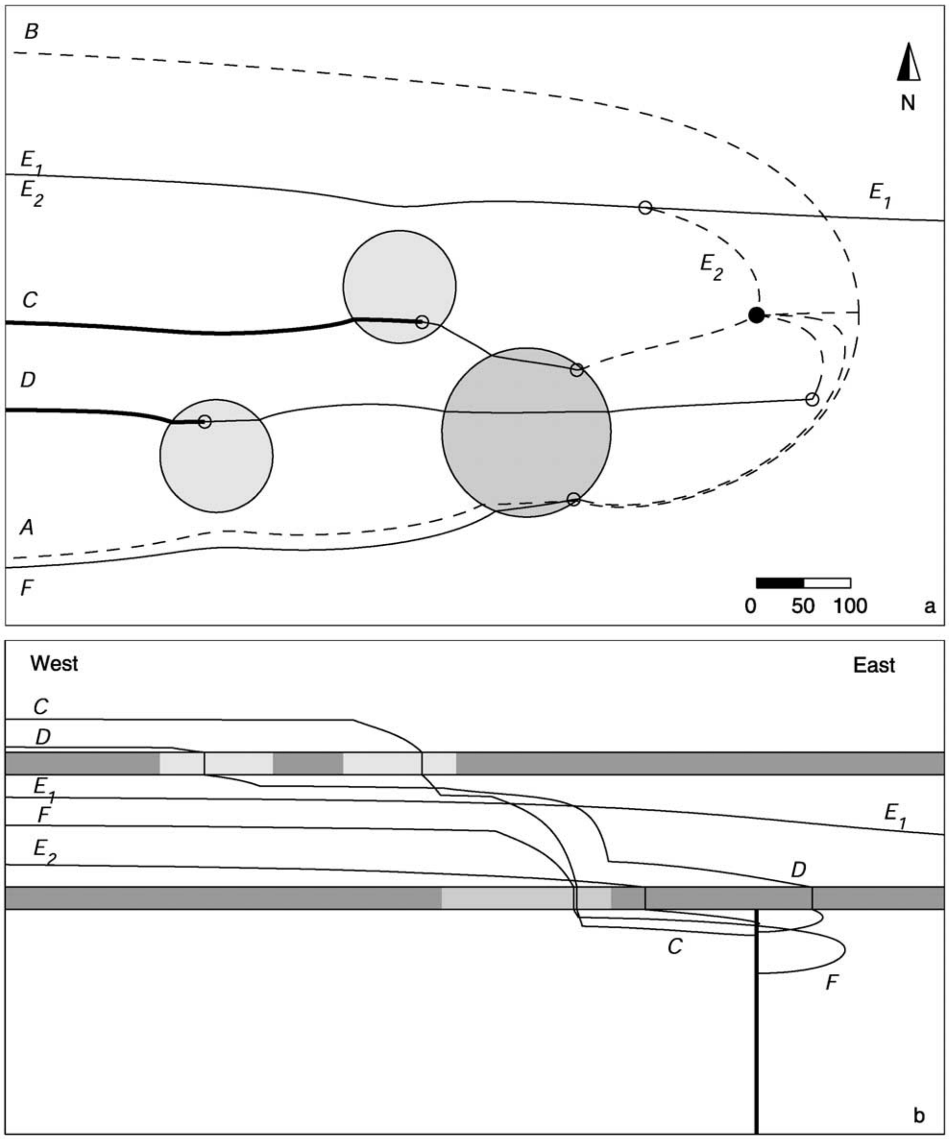

Fig. 3. Application II. (a) Horizontal projection of pathlines in top aquifer (thick), middle aquifer (thin), and bottom aquifer (dashed), (b) Projection of pathlines on West–East vertical cross-section (vertical scale exaggerated).

show a significant deviation from the other pathlines. The cylindrical inhomogeneities in the top aquifer cause a significant lateral spreading of the tracer.

8. Application II

The second application concerns flow towards a well screened in the bottom aquifer of a confined aquifer system with three aquifers and two leaky clay layers. The three aquifers are homogeneous, but the two clay layers have cylindrical holes of smaller vertical resistance. The thickness of the top two aquifers is 10 m each, the thickness of the bottom aquifer is 20 m, and the hydraulic conductivity of all aquifers is 2 m/d. There are two holes of radius 60 m in the top clay layer (light gray circles in Fig. 3(a)) and one hole of radius 80 m in the bottom clay layer (dark

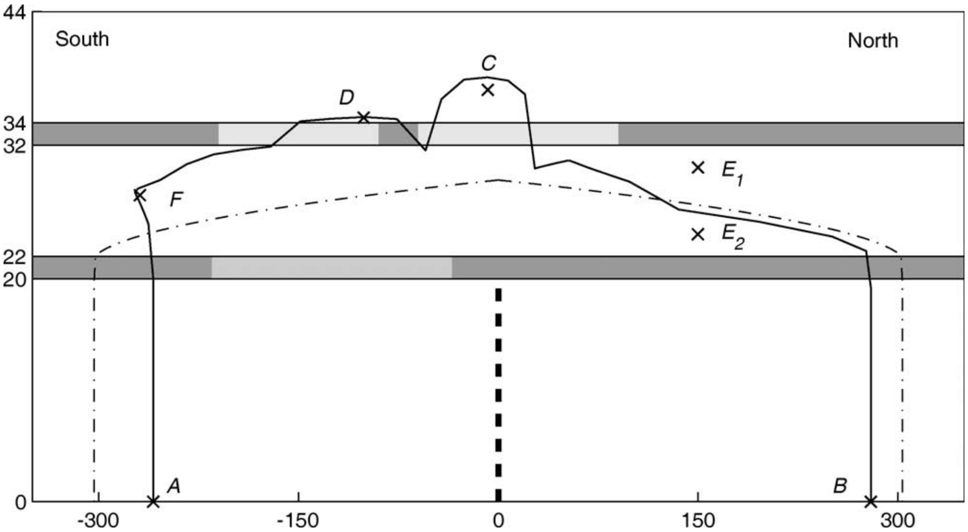

Fig. 4. Application II. South–North vertical cross section 800 m upstream of well (vertical scale exaggerated). Thick line represents boundary of capture zone envelope. Dashed-dotted line is capture zone envelope in absence of holes.

gray, larger circle in Fig. 3(a)). The resistance to vertical flow of the clay layers is 10,000 d, except for inside the cylindrical holes where it is 50 d. Far away from the well, flow is uniform from West to East with a gradient of 0.01; the discharge of the well is 300 m^3/d. The effect of the well is represented by the analytic solution for flow to a well in a multi-aquifer system (e.g. Hemker, 1984; Bakker, 2001).

Seven pathlines are shown in Fig. 3. Fig. 3(a) represents a plan view and Fig. 3(b) is a projection of the pathlines on a West–East running vertical plane. In Fig. 3(a), a thick solid line represents a pathline in the top aquifer, a thin solid line a pathline in the middle aquifer, and a dashed line a pathline in the bottom aquifer. A small circle is drawn at the point where a pathline leaks to a lower aquifer. All pathlines are started 800 m upstream of the well. A vertical South–North cross-section, 800 m upstream of the well, is shown in Fig. 4. The thick solid line represents the capture zone envelope and the crosses indicate the starting points of the pathlines. The dashed-dotted line represents the capture zone envelope in absence of the holes in the leaky layers.

Pathlines *A* and *B* are started at the bottom of the aquifer system and represent the capture zone envelope in the bottom aquifer. When a pathline is started in any of the top two aquifers and leaks to the bottom aquifer between pathlines *A* and *B*, then the pathline will end at the well; otherwise it will bypass the well. The capture zone envelope extends to the top aquifer due to the presence of the holes in the leaky layers. For example, pathlines *C* and *D* are started in aquifer 1 and end at the well. It may be seen from Fig. 3 that pathlines *C* and *D* were started within the three-dimensional capture zone envelope. At point *E*, two pathlines are started at different elevations; pathline E_1 starts outside the capture zone envelope and pathline E_2 starts inside the capture zone envelope. The two pathlines follow the same path in the horizontal plane until pathline E_2 leaks to the bottom aquifer. It may be interesting to point out that the horizontal extent of the capture zone envelope may be larger in the middle aquifer than in the bottom aquifer. This is illustrated by pathline *F*, which is started in the middle aquifer outside the horizontal extend of the capture zone envelope in the bottom aquifer, but it still ends at the well, because it leaks to the bottom aquifer between pathlines *A* and *B*.

9. Conclusions

A new approach was presented for the simulation of steady groundwater flow in multi-aquifer systems with many cylindrical inhomogeneities.

The properties of all aquifers and leaky layers may be different inside each cylinder. The approach is limited to cases where flow remains (semi)confined in all aquifers; cylinders may not overlap. Solutions obtained with the new approach fulfill the system of differential equations exactly and fulfill the boundary conditions along the boundary of the cylinder up to any desired accuracy (depending on the abilities of the employed computer). For simplicity, the analysis was restricted to the case where the number of aquifers and leaky layers on the outside of the cylinder was equal to the number on the inside of the cylinder. This is not a limitation of the approach, which may equally well be applied to cylindrical inhomogeneities consisting of an arbitrary number of aquifers.

The head, flow and leakage may be computed analytically at any point in the aquifer system. The practical significance of the proposed approach was illustrated by the presentation of two hypothetical applications. In the first application, flow was considered in a two aquifer system with cylindrical inhomogeneities in the top aquifer only; the bottom aquifer was homogeneous. It was shown that a conservative tracer that is released in the bottom aquifer is subject to a significant lateral spreading due to the inhomogeneities in the overlying aquifer. In the second application, the capture zone of a pumping well in a three-aquifer system was evaluated. The effect of cylindrical holes of lower resistance in the leaky clay layers was evaluated. It was shown that the cylindrical holes caused the capture zone of the well to extend all the way to the top aquifer.

Appendix

The radial and tangential components of the discharge vector are obtained with Eq. (7). The radial discharge outside the cylinder is

$$\vec{Q}_r = \sum_{p=1}^{P} [a_p\cos(p\theta) + b_p\sin(p\theta)]\frac{p}{r^{p+1}}\vec{T}_n - \sum_{m=1}^{M-1}\sum_{p=0}^{P}[c_{p,m}\cos(p\theta) + d_{p,m}\sin(p\theta)]\mathrm{K}'_\mathrm{p}(r/\Lambda_m)\vec{U}_m \tag{31}$$

and inside the cylinder

$$\vec{Q}_r = -\sum_{p=1}^{P}[\alpha_p\cos(p\theta)+\beta_p\sin(p\theta)]pr^{p-1}\vec{\tau}_n - \sum_{m=1}^{M-1}\sum_{p=0}^{P}[\gamma_{p,m}\cos(p\theta)+\delta_{p,m}\sin(p\theta)]\mathrm{I}'_\mathrm{p}(r/\lambda_m)\vec{V}_m \tag{32}$$

where the prime stands for differentiation with respect to r. The derivatives of the Bessel functions are (e.g. Abramowitz and Stegun, 1969)

$$\mathrm{I}'_\mathrm{p}(r/\lambda_m) = \frac{\mathrm{I}_{\mathrm{p}-1}(r/\lambda_m)+\mathrm{I}_{\mathrm{p}+1}(r/\lambda_m)}{2\lambda_m} \tag{33}$$

$$\mathrm{K}'_\mathrm{p}(r/\Lambda_m) = -\frac{\mathrm{K}_{\mathrm{p}-1}(r/\Lambda_m)+\mathrm{K}_{\mathrm{p}+1}(r/\Lambda_m)}{2\Lambda_m} \tag{34}$$

The tangential discharge outside the cylinder is

$$\vec{Q}_\theta = \sum_{p=1}^{P}[a_p\sin(p\theta) - b_p\cos(p\theta)]\frac{p}{r^{p+1}}\vec{T}_n + \sum_{m=1}^{M-1}\sum_{p=1}^{P}[c_{p,m}\sin(p\theta) - d_{p,m}\cos(p\theta)]\frac{p}{r}\mathrm{K}_\mathrm{p}(r/\Lambda_m)\vec{U}_m \tag{35}$$

and inside the cylinder

$$\vec{Q}_\theta = \sum_{p=1}^{P}[\alpha_p\sin(p\theta)+\beta_p\cos(p\theta)]pr^{p-1}\vec{\tau}_n + \sum_{m=1}^{M-1}\sum_{p=1}^{P}[\gamma_{p,m}\sin(p\theta) - \delta_{p,m}\cos(p\theta)]\frac{p}{r}\mathrm{I}_\mathrm{p}(r/\lambda_m)\vec{V}_{\vec{m}} \tag{36}$$

References

Abramowitz, M., Stegun, I.A., 1965. Handbook of Mathematical Functions, Dover Publications, New York.

Bakker, M., 2001. An analytic, approximate method for modeling steady, three-dimensional flow to partially penetrating wells. Water Resources Research 37 (5), 1301–1308.

Bakker, M., 2002. Two exact solutions for a cylindrical inhomogeneity in a multi-aquifer system. Advances in Water Resources 25 (1), 9–18.

Bakker, M., Strack, O.D.L., 2003. Analytic elements for multi-aquifer flow. Journal of Hydrology 271 (1–4), 119–129.

Barnes, R., Janković, I., 1999. Two-dimensional flow through large numbers of circular inhomogeneities. Journal of Hydrology 226 (3–4), 204–210.

Bruggeman, G.A., 1999. Analytical solutions of geohydrological problems, Developments in Water Science, 46. Elsevier, Amsterdam.

Fitts, C.R., 1991. Modeling three-dimensional flow about ellipsoidal inhomogeneities with application to flow to a gravel-packed well and flow through lens-shaped inhomogeneities. Water Resources Research 21 (10), 1557–1566.

Haitjema, H.M., 1995. Analytic Element Modeling of Groundwater Flow, Academic Press, San Diego, CA.

Hemker, C.J., 1984. Steady groundwater flow in leaky multiple-aquifer systems. Journal of Hydrology 72, 355–374.

Janković, I., Barnes, R., 1999. Three-dimensional flow through large numbers of spheroidal inhomogeneities. Journal of Hydrology 226 (3–4), 224–233.

Maas, C., 1986. The use of matrix differential calculus in problems of multiple-aquifer flow. Journal of Hydrology 99, 43–67.

Magnus, J.R., Neudecker, H., 1999. Matrix Differential Calculus with Applications in Statistics and Economics, Wiley, New York, Revised edition.

Moon, P., Spencer, D.E., 1971. Field Theory Handbook : Including Coordinate Systems, Differential Equations and Their Solutions, Second ed, Springer, New York, NY.

Polubarinova-Kochina, P., 1962. Theory of Groundwater Movement, Princeton University Press, Princeton, NJ, translated by J.M.R. de Wiest.

Strack, O.D.L., 1981. Flow in aquifers with clay lamina, 1. The comprehensive potential. Water Resources Research 17 (4), 985–992.

Strack, O.D.L., 1984. Three-dimensional streamlines in Dupuit–Forchheimer models. Water Resources Research 20 (7), 812–822.

Strack, O.D.L., 1987. The analytic element method for regional groundwater modeling. Proceedings National Water Well Association, Conference on Solving Groundwater Problems with Models, Denver, CO, February 10–12, 1987, 929–941.

Strack, O.D.L., 1989. Groundwater Mechanics, Prentice Hall, Englewood Cliffs, NJ.